PHYSICAL REVIEW B VOLUME 60, NUMBER 22 1 DECEMBER 1999-II

# Magnetism in $La_{8-x}Sr_xCu_8O_{20}$: A hybrid system with localized one-dimensional Cu-O chains and an itinerant three-dimensional Cu-O network

T. Ito, H. Yamaguchi, and K. Oka
*Electrotechnical Laboratory, 1-1-4 Umezono, Tsukuba, Ibaraki 305-8568, Japan*

K. Nozawa and H. Takagi
*ISSP, The University of Tokyo, 7-22-1 Roppongi, Minato-ku, Tokyo 106-8666, Japan*

(Received 25 August 1999)

The oxygen deficient perovskite $La_{8-x}Sr_xCu_8O_{20}$ is unique in that the system can be viewed as a hybrid of parallel one-dimensional chains with localized $S=1/2$ spins and surrounding three-dimensional Cu-O network with itinerant electrons. For $x \lesssim 2.1$, two successive phase transitions are observed, where complicated anomalies appear in magnetic and transport properties. We discuss the roles of these two subsystems in the complicated magnetism of the present compound. [S0163-1829(99)50746-7]

Complex copper oxides crystallize in a variety of modified perovskite structures. This structural variety gives rise to surprisingly rich physical properties, which has been providing fresh fuel to the field of condensed-matter physics. High-$T_c$ superconductivity is realized in layered cuprates with two-dimensional $CuO_2$ planes. One-dimensional (1D) cuprates with Cu-O chains such as $Sr_2CuO_3$ and $SrCuO_2$ form ideal 1D $S=1/2$ Heisenberg antiferromagnets and give us unique opportunities to examine quantum spin liquid states.[1] Stimulated by theoretical proposals,[2] spin ladder compounds have been explored extensively and superconductivity was achieved in $(Sr,Ca)_{14}Cu_{24}O_{41}$,[3] though the connection between the theoretical proposals and the observed superconductivity is not yet evident.[4]

The oxygen deficient perovskite $La_{8-x}Sr_xCu_8O_{20}$ has been known to be metallic but not superconducting.[5] The crystal structure of $La_{8-x}Sr_xCu_8O_{20}$, determined by Er-Rakho *et al.*,[6] is shown in Fig. 1. The symmetry is tetragonal, with the lattice constants $a_0=10.840$ Å and $c_0=3.861$ Å for $x=1.60$.[6,7] The essential difference from the original perovskite structure is the presence of ordered oxygen vacancies running parallel to the $c$ axis, which gives rise to arrays of Cu-O units of $CuO_4$ planar squares, $CuO_5$ pyramids, and $CuO_6$ octahedra. In view of the oxygen coordination number, it is highly likely that carriers are mainly doped into the octahedral and the pyramidal sites, rather than the square sites. Using bond valence sum calculation,[8] formal Cu valences for $x=1.6$ are indeed estimated to be $+2.4$, $+2.5$, and $+2.1$ for the octahedral, the pyramidal, and the square sites, respectively. The $CuO_6$ octahedra are only slightly distorted and a substantial admixture of the Cu $3d_{3z^2-r^2}$ character at the Fermi level is expected. This will help to establish a sizeable coupling between the octahedral and the pyramidal sites, leading to a three-dimensional (3D) character of doped holes predominantly spreading over the octahedra and the pyramids. On the other hand, the square sites with substantially fewer number of holes than the other two sites would be insulating and can be viewed as $S=1/2$ Heisenberg chains with a large antiferromagnetic intrachain coupling $J$ as usually found in corner-sharing Cu-O chains.[1] This oxygen deficient perovskite is therefore very unique in that a hybrid of the 1D $S=1/2$ Heisenberg chains and the itinerant 3D Cu-O network is realized.

Since the $d_{x^2-y^2}$ orbitals of neighboring square and pyramidal sites are orthogonal to each other, the spin chains and the itinerant electron system are only weakly coupled.[9] However, this weak coupling may potentially have a substantial influence, because 1D spin Heisenberg chains are highly sensitive to small perturbations. Interplay between the localized moments on the chains and the conduction electrons and resultant magnetism may therefore be expected. In the past, magnetic and transport anomalies were reported for $x \sim 1.5$ samples, but details have not been explored yet, partly because of the lack of homogeneous single crystalline samples.[5] We therefore have grown a series of single crystals of $La_{8-x}Sr_xCu_8O_{20}$ with well-controlled Sr contents and investigated their transport and magnetic properties. We observed a presence of two distinct magnetic metallic phases at low temperatures and found systematic suppression of the transitions into these phases with increasing $x$ from 1.5. We discuss that the complicated magnetism very likely origi-

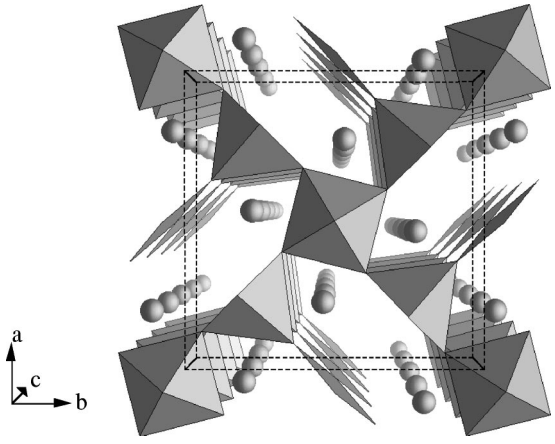


FIG. 1. Perspective view of the crystal structure of $La_{8-x}Sr_xCu_8O_{20}$. The spheres depict La or Sr atoms, and the polyhedra depict Cu and surrounding O atoms. The dashed lines show the unit cell. The atomic positions are taken from Ref. 6.

 

nates from coexistence of and interplay between the localized 1D chain spins and the 3D itinerant electrons.

Single crystals of $La_{8-x}Sr_xCu_8O_{20}$ in a range of $x=1.50$–$2.24$ were successfully grown by the traveling-solvent floating-zone (TSFZ) method.[10] This compound is reported to melt incongruently.[11] We therefore used nonstoichiometric solvent with an empirically determined cation ratio of La:Sr:Cu$=1-x/8:x/8:3$. The growth was performed in oxygen under a pressure of 0.2–0.4 MPa, with a growth rate of 0.5 mm/h. Thus obtained crystals had a cylindrical shape with typical dimensions of 4 mm $\phi\times 50$ mm and a $c$ axis parallel to the rod axis. (On the cylinder, four facets are sometimes observed, reflecting tetragonal symmetry.) The Sr content $x$ of the crystals was determined by the inductively coupled plasma atomic emission spectroscopy (ICP-AES). Two sets of rectangular-shaped samples with [110] and [001] along the longest dimension were cut from the crystal rods for anisotropic transport measurements. Resistivity was measured using a conventional four-terminal method. Magnetization was measured using a superconducting quantum interference device (SQUID) magnetometer in magnetic fields up to $H=5$ T.

The transport and the magnetic properties of the single crystals with a representative composition $x=1.60$ are summarized in Fig. 2. The top panel demonstrates the temperature-dependent resistivities with current parallel to the chain ($\|[001]$) and perpendicular to the chain ($\|[110]$), $\rho_{[001]}$ and $\rho_{[110]}$. As is evident from the figure, both $\rho_{[001]}$ and $\rho_{[110]}$ are metallic down to $T=2$ K with a moderate anisotropy ratio $\rho_{[110]}/\rho_{[001]}\sim 8$–$9$. Therefore, $La_{8-x}Sr_xCu_8O_{20}$ can be classified as an anisotropic 3D metal, revealing a presence of 3D network with itinerant electrons very likely originating from the octahedral and the pyramidal sites. Two clear anomalies, indicative of phase transitions, are observed at $T=145$ K ($T_{c1}$) and 85 K ($T_{c2}$), which can be seen as kinks in $\rho(T)$ in the top panel of Fig. 2. At $T=T_{c1}$, the anomaly is more pronounced in $\rho_{[001]}(T)$ than in $\rho_{[110]}(T)$, whereas, at $T=T_{c2}$, it is significant only for $\rho_{[110]}(T)$. No noticeable hysteresis as a function of temperature was observed at these two transitions.

These two transitions manifest themselves in distinctly different ways in the Hall effect. The second panel of Fig. 2 demonstrates the temperature dependence of the anisotropic Hall coefficient $R_{H,[110]}$ and $R_{H,[001]}$ for $x=1.60$, with magnetic field applied parallel to [110] and [001] and current parallel to [001] and [110], respectively. The sign was found to be negative for both $R_{H,[110]}$ and $R_{H,[001]}$, which contrasts with that of the high-$T_c$ layered cuprates with a similar hole concentration. We observe a drastic change of $R_H$ only at $T_{c2}\sim 85$ K. Below $T=T_{c2}$, $R_{H,[110]}$ and $R_{H,[001]}$ first show a rapid decrease and increase, respectively, and then saturate eventually at the $T=0$ limit. Any appreciable anomalies were not observed at $T_{c1}\sim 145$ K for both $R_{H,[110]}$ and $R_{H,[001]}$. These contrasted behaviors in $R_H$ at the two transitions suggest that, while the transition at $T=T_{c1}$ mainly originates from a change in the scattering channel, the transition at $T=T_{c2}$ is associated with a drastic reconstruction of the Fermi surface.

Pronounced and anisotropic anomalies in the magnetization are observed both at $T=T_{c1}$ and $T_{c2}$, indicating that these transitions are accompanied with magnetic orderings.

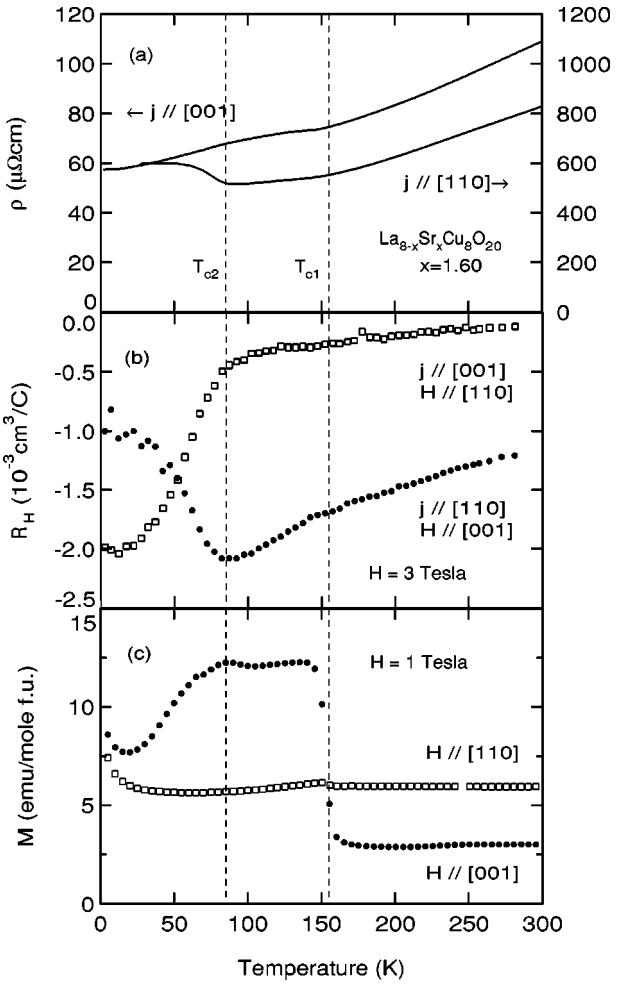


FIG. 2. Temperature dependences of the anisotropic (a) resistivity $\rho$, (b) Hall coefficient $R_H$, and (c) magnetization $M$ of $La_{8-x}Sr_xCu_8O_{20}$ ($x=1.60$). The dashed lines represent the magnetic transition temperatures $T_{c1}$ and $T_{c2}$ determined by the magnetization measurements. A part where $\rho$ is affected by superconductivity in $La_{2-x}Sr_xCuO_4$ is not shown.

A preliminary muon spin relaxation ($\mu$SR) experiment indeed indicates a presence of ordered moments in the whole temperature range below $T=T_{c1}$, including the range below $T=T_{c2}$.[12] The temperature-dependent magnetizations with $H\|[001]$ and [110] at $H=1$ T, $M_{[001]}$ and $M_{[110]}$, are presented in the bottom panel of Fig. 2. $M_{[001]}$ is almost temperature-independent above $T=T_{c1}$. With decreasing temperature, it shows an abrupt increase at $T=T_{c1}$ and then shows an abrupt decrease at $T=T_{c2}$. As shown in the inset of Fig. 3, in the temperature range between $T=T_{c1}$ and $T_{c2}$, $M_{[001]}$ is nonlinear in $H$ with small hysteresis, revealing an existence of weak ferromagnetic spontaneous moments. The size of the moments is estimated to be $\sim 30$ emu/mole f.u. from linear extrapolation of the data at high fields, which is about 3 orders of magnitude smaller than those expected for $Cu^{2+}$ spins with $S=1/2$ and $g=2$. In the temperature range below $T=T_{c2}$, $M_{[001]}$ is linear in $H$. In contrast, $M_{[110]}$ is very weakly temperature dependent and shows kinks at the two transitions. We found that $M_{[110]}$ is always $H$ linear at any temperatures, in contrast with $M_{[001]}$. These results indicate that the metallic single crystals with $x=1.60$ experience two successive magnetic transitions, first from a para-

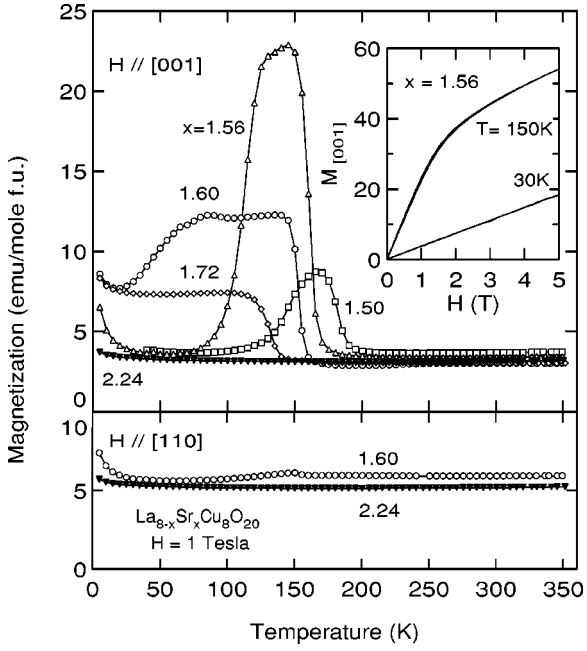


FIG. 3. Temperature dependence of anisotropic magnetization $M$ of $La_{8-x}Sr_xCu_8O_{20}$ with various Sr contents. The parts where $M$ is affected by superconductivity in $La_{2-x}Sr_xCuO_4$ in some samples are not shown. The inset: magnetization $M_{[001]}$ as a function of a magnetic field $H$ for $x=1.56$ at two representative temperatures.

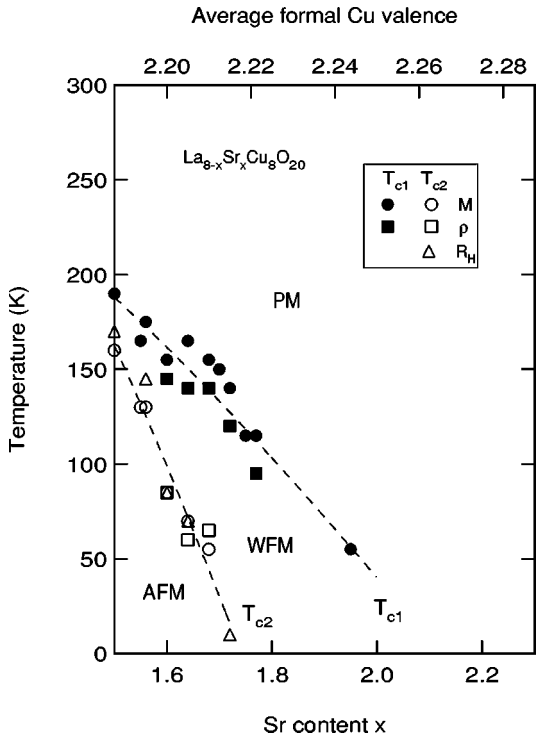


FIG. 4. Phase diagram of $La_{8-x}Sr_xCu_8O_{20}$, determined by the anomalies in magnetization, resistivity, and Hall coefficient. $T_{c1}$ and $T_{c2}$ denote magnetic transition temperatures. PM, WFM, and AFM denote a paramagnetic metallic, a weakly ferromagnetic metallic, and an antiferromagnetic metallic phase, respectively. The dashed lines are guides to the eye.

magnet (PM) to a weak ferromagnet (WFM) at $T=T_{c1}$ and then from the WFM to an antiferromagnet (AFM) at $T=T_{c2}$.

These two magnetic phase transitions at low temperatures are suppressed by increasing Sr content and eventually disappear. In Fig. 3, the temperature-dependent magnetizations for the single crystals with various Sr contents are shown. As clearly seen from the figure, two magnetic transition temperatures, represented by an abrupt increase and decrease, show systematic decrease with increasing Sr content from $x=1.5$, and eventually disappear. Above $x=2.1$, the magnetization is almost temperature independent and shows no trace of anomaly, indicating that a paramagnetic ground state is finally realized. The doping dependence can be visually summarized as a phase diagram in Fig. 4, which shows the transition temperatures obtained from the magnetization (shown in Fig. 3) together with those obtained from the resistivity and the Hall effect. The transition temperatures are defined as the kink temperatures for the resistivity and the Hall effect and the temperatures where $M_{[001]}$ begins to increase or decrease. The data are plotted in Fig. 4, only when the transition is well defined. Although there exists a certain ambiguity in defining the transition temperatures, all the transition temperatures obtained from different sources agree reasonably, confirming all the observed anomalies commonly originate from the two phase transitions. In the phase diagram, $T_{c2}$ decreases rapidly with hole doping, suggestive of instability of the AFM phase. It is noticeable from the phase diagram that, as a function of doping level, the ground state changes from the AFM metal to the WFM metal at $x\sim1.7$ and then to the PM metal at $x\sim2.1$ and that there exist two magnetic critical points. The details of the critical behavior will be discussed in the next paper.

The contrasted behaviors of the Hall effect between the AFM and the WFM phases indicate that the appreciable reconstruction of the Fermi surface occurs only in the former. Therefore, to understand these two successive phase transitions as a function of temperature and doping level, it is natural to invoke explicitly the presence of two subsystems expected from the unique crystal structure, namely highly localized 1D Heisenberg chains and 3D networks of Cu-O octahedra and pyramids with itinerant holes. Almost $T$-independent magnetic susceptibility in the PM phase does not contradict the presence of the chain with localized spins, since the 1D Heisenberg antiferromagnet shows a weakly $T$-dependent susceptibility below $T\sim J$ (presumably $\sim2000$ K). In this context, we propose the following scenario for the observed phase transitions. In the AFM phase, the Fermi surface, with the predominant character of the Cu-O octahedra and pyramids, experiences spin density wave (SDW) formation and therefore is partially gapped, which gives rise to the drastic change of the Hall effect. It may be informative to infer that our preliminary neutron-diffraction study revealed an appearance of incommensurate peaks only in the AFM phase,[13] which may arise from the Fermi surface nesting. In contrast, in the WFM phase, the highly localized 1D Heisenberg chains play a dominant role in the magnetic ordering and the conduction electrons experience only a modest change. It is natural that the 1D antiferromagnetic Heisenberg chains with a finite interchain coupling order antiferromagnetically. With increasing $x$, it is likely that carriers are finally doped into the 1D chains and the chains become itinerant, which results in the suppression of $T_{c1}$. The condition of the Fermi surface nesting in the 3D itinerant electron sys-

tem would be sensitive to the hole concentration, which may be related to the rapid suppression of $T_{c2}$.

Weak but finite coupling between the 1D chain spins and the 3D electrons, which may affect the magnetism of the system seriously, is expected for the present system. In conventional quasi-1D Heisenberg antiferromagnets such as $Sr_2CuO_3$, interchain coupling, necessary for magnetic ordering, originates from weak superexchange interaction. In contrast, interchain coupling in the present system originates partly from mediation by the 3D itinerant electron system in addition to the conventional weak superexchange interaction. If the former interchain interaction with a dynamic character is dominant, the coherence and dynamics of magnetic ordering along the inter- and the intrachain directions are expected to be very anisotropic or substantially different. This unique coupling between the 1D spins and the 3D electrons may also be related to the anomalous weakly ferromagnetic moments, which appear only in the WFM phase, but not in the AFM phase.

In summary, we show a systematic study on magnetic and transport properties of $La_{8-x}Sr_xCu_8O_{20}$ ($x=1.50$–$2.24$) single crystals. We found two sets of anomalies for $x \lesssim 2.1$, which correspond to successive magnetic transitions into weakly ferromagnetic metallic and antiferromagnetic metallic phases. A significant feature in the weakly ferromagnetic phase is an emergence of weak ferromagnetic moments, whereas that in the antiferromagnetic one is an anisotropic change of transport properties such as Hall effect, suggesting a drastic reconstruction of the Fermi surface. The transitions into these magnetic phases are suppressed with increasing $x$. We propose that these complicated magnetic transitions originate from a unique structural aspect of this oxygen deficient perovskite, namely, a hybrid of parallel 1D Heisenberg chains with localized $S=1/2$ spins and a surrounding 3D Cu-O network with a substantial number of itinerant holes.

We are grateful to K. Yamaji, G. Aeppli, K. M. Kojima, T. Yanagisawa, Y. Shimoi, and T. Takimoto for stimulating discussions, and to M. Tokumoto for support of magnetization measurements.

[1] N. Motoyama, H. Eisaki, and S. Uchida, Phys. Rev. Lett. **76**, 3212 (1996); K. M. Kojima *et al.*, *ibid.* **78**, 1787 (1997).

[2] E. Dagotto, J. Riera, and D. Scalapino, Phys. Rev. B **45**, 5744 (1992).

[3] M. Uehara *et al.*, J. Phys. Soc. Jpn. **65**, 2764 (1996).

[4] T. Nagata *et al.*, Phys. Rev. Lett. **81**, 1090 (1998).

[5] J. B. Torrance *et al.*, Phys. Rev. Lett. **60**, 542 (1988); T. Tamegai and Y. Iye, Physica C **159**, 181 (1989); T. Watanabe and A. Matsuda, Jpn. J. Appl. Phys., Part 2 **30**, L985 (1991); Y. Enomoto *et al.*, Phys. Rev. B **42**, 6773 (1990).

[6] L. Er-Rakho, C. Michel, and B. Raveau, J. Solid State Chem. **73**, 514 (1988).

[7] Doubling of $c_0$ in a wide $x$ and temperature region is observed by x-ray- and electron-diffraction experiments, indicating the presence of a structural transition [H. Yamaguchi *et al.*, Physica C **282-287**, 1079 (1997); F. Matsuhata *et al.*, in *Proceedings of the 14th International Congress on Electron Microscopy*, edited by H. Calderon and M. J. Yacaman (IOP, Bristol, 1998), Vol. 2, p. 785. We found no traces of magnetic dimerization in magnetic and transport properties at this structural transition temperature. The magnetic orderings occur in the doubled structural unit cell. We do not consider the effect of this structural transition in this paper.

[8] I. D. Brown and D. Altermatt, Acta Crystallogr., Sect. B: Struct. Sci. **B41**, 244 (1985).

[9] The local structure in which the squares are sandwiched by the pyramids is similar to that in $YBa_2Cu_3O_7$, where the hybridization between their orbitals is very small [J. Yu *et al.*, Phys. Lett. A **122**, 203 (1987)]. For $La_{8-x}Sr_xCu_8O_{20}$, the distance between a Cu atom at the pyramid (square) site and an O atom shared by these two Cu atoms is 0.09 (0.06) Å longer than that for $YBa_2Cu_3O_7$ [M. A. Beno *et al.*, Appl. Phys. Lett. **51**, 57 (1987)], which would make their hybridization in $La_{8-x}Sr_xCu_8O_{20}$ weaker.

[10] T. Ito, H. Yamaguchi, and K. Oka, Chin. J. Low Temp. Phys. **19**, 36 (1997).

[11] K. Otzschi, A. Hayashi, and Y. Ueda, J. Supercond. **7**, 73 (1994).

[12] T. Ito, K. M. Kojima, B. Nachumi, and Y. J. Uemura, Physica B (to be published).

[13] T. Ito, C. H. Lee, M. Takahashi, and M. Arai (unpublished).